HEPATOLOGY

HEPATOLOGY, VOL. 70, NO. 4, 2019

Dual Specificity Phosphatase 12 Regulates Hepatic Lipid Metabolism Through Inhibition of the Lipogenesis and Apoptosis Signal–Regulating Kinase 1 Pathways

Zhen Huang,[1*] Lei-Ming Wu,[1*] Jie-Lei Zhang,[2*] Abdelkarim Sabri,[3] Shou-Jun Wang,[2] Gui-Jun Qin,[2] Chang-Qing Guo,[4] Hong-Tao Wen,[4] Bin-Bin Du,[1] Dian-Hong Zhang,[1] Ling-Yao Kong,[1] Xin-Yu Tian,[1] Rui Yao,[1] Ya-Peng Li,[1] Cui Liang,[1] Peng-Cheng Li,[1] Zheng Wang,[1] Jin-Yan Guo,[5] Ling Li,[1] Jian-Zeng Dong,[1] and Yan-Zhou Zhang[1]

Nonalcoholic fatty liver disease (NAFLD) has become the most common cause of chronic liver disease worldwide. Due to the growing economic burden of NAFLD on public health, it has become an emergent target for clinical intervention. DUSP12 is a member of the dual specificity phosphatase (DUSP) family, which plays important roles in brown adipocyte differentiation, microbial infection, and cardiac hypertrophy. However, the role of DUSP12 in NAFLD has yet to be clarified. Here, we reveal that DUSP12 protects against hepatic steatosis and inflammation in L02 cells after palmitic acid/oleic acid treatment. We demonstrate that hepatocyte specific DUSP12-deficient mice exhibit high-fat diet (HFD)–induced and high-fat high-cholesterol diet–induced hyperinsulinemia and liver steatosis and decreased insulin sensitivity. Consistently, DUSP12 overexpression in hepatocyte could reduce HFD-induced hepatic steatosis, insulin resistance, and inflammation. At the molecular level, steatosis in the absence of DUSP12 was characterized by elevated apoptosis signal-regulating kinase 1 (ASK1), which mediates the mitogen-activated protein kinase (MAPK) pathway and hepatic metabolism. DUSP12 physically binds to ASK1, promotes its dephosphorylation, and inhibits its action on ASK1-related proteins, JUN N-terminal kinase, and p38 MAPK in order to inhibit lipogenesis under high-fat conditions. *Conclusion:* **DUSP12 acts as a positive regulator in hepatic steatosis and offers potential therapeutic opportunities for NAFLD. (Hepatology 2019;70:1099-1118).**

SEE EDITORIAL ON PAGE 1091

Nonalcoholic fatty liver disease (NAFLD) is the most common diffuse liver disease and is characterized by lipid accumulation in hepatocytes in the absence of excessive alcohol consumption.[1] The prevalence of NAFLD increases worryingly with obesity and other diseases of metabolic syndrome (MS) and is expected to be the leading cause of liver failure in the future.[2] Accumulating studies show that NAFLD not only is linked to an increased risk of liver-related mortality or morbidity

Abbreviations: ACACα, acetyl-coenzyme A carboxylase α; ALT, alanine aminotransferase; ASK1, apoptosis signal–regulating kinase 1; AST, aspartate aminotransferase; BSA, bovine serum albumin; CCL2, chemokine (C-C motif) ligand 2; CD, cluster of differentiation; CKO, hepatocyte-specific DUSP12 knockout (mice); CPT1a, carnitine palmitoyltransferase 1a; DUSP, dual specificity phosphatase; FASN, fatty acid synthase; G6PC, glucose-6-phosphatase; GST, glutathione S-transferase; GTT, glucose tolerance test; HA, hemagglutinin; H&E, hematoxylin and eosin; HFD, high-fat diet; HFHC, high-fat high-cholesterol (diet); IKBα, inhibitor of kappa light polypeptide gene enhancer in B cells; IKKβ, inhibitor of NF-κB kinase subunit beta; IL, interleukin; IP, immunoprecipitation; IR, insulin resistance; ITT, insulin tolerance test; JNK, JUN N-terminal kinase; MAPK, mitogen-activated protein kinase; MKK, MAPK kinase; NAFLD, nonalcoholic fatty liver disease; NASH, nonalcoholic steatohepatitis; NC, normal chow; NEFA, nonesterified fatty acid; NF-κB, nuclear factor kappa B; NTG, nontransgenic; OA, oleic acid; PA, palmitic acid; PCK1, gluconeogenesis phosphoenolpyruvate carboxykinase 1; PPARγ, peroxisome proliferator–activated nuclear receptor gamma; SCD-1, stearoyl-coenzyme A desaturase-1; si, small interfering; TC, total cholesterol; TG, transgenic; TNF-α, tumor necrosis factor alpha.

Received October 17, 2018; accepted February 13, 2019.

Additional Supporting Information may be found at onlinelibrary.wiley.com/doi/10.1002/hep.30597/suppinfo.

**These authors contributed equally to this work.*

Supported by grants from the National Natural Science Foundation of China (81770048) and the Cooperative Project of Academy Training Foundation of Zhengzhou University (2016-BSTDJJ-13).

but also affects some extrahepatic organs, including the cardiovascular and renal systems, as a multisystemic disease.[3] Due to the growing economic burden of NAFLD on public health, it has become an emergent target for clinical intervention.[4] While tremendous progress has been made over the last decade in investigating the pathogenesis of NAFLD and developing treatment strategies, the development of additional tasks of therapeutics is urgently needed to further reduce the burden of NAFLD.

Naturally, NAFLD is a heterogeneous disease, and a full understanding of the mechanisms contributing to progression risk in NAFLD is vital for providing clarity in this regard. The spectrum of NAFLD ranges from simple steatosis to advanced stages, including nonalcoholic steatohepatitis (NASH), hepatic fibrosis, and cirrhosis.[5-7] Different theories have been pointed out, leading initially to the "two-hit hypothesis." The first hit is insulin resistance (IR) and lipotoxicity causing hepatocyte injury, but a second hit is needed for chronic liver damage and includes apoptosis, oxidative stress, and lipid peroxidation.[8] In patients with NAFLD, both environmental and genetic factors are involved in the insulin signaling pathway and therefore contribute to the maintenance and worsening of IR, inflammation, and fibrosis. At the molecular level, the mechanism underlying the development and progression of NAFLD is complex and multifactorial. Multiple signaling pathways have been reported to be involved in the dynamic regulation of NAFLD, including mitogen-activated protein kinases (MAPKs) and nuclear factor kappa B (NF-κB).[9] Thus, an in-depth understanding of the molecular basis of NAFLD is required to explore effective therapeutic targets.[10-12]

Dual-specificity phosphatases (DUSPs) are members of a family of proteins that specifically dephosphorylates threonine and tyrosine residues.[13] DUSP12 is a member of a subgroup of atypical DUSPs that contain a zinc finger domain, a consensus DUSP catalytic domain, and a highly conserved aldehyde dehydrogenase cysteine active site.[14] Because DUSP12 was identified in 2005 by a small interfering RNA (siRNA) screen, its function has been poorly explored.[15] It was reported as a prosurvival phosphatase that is involved in cancer by regulating ribosome biogenesis and cell cycle progression.[16] Additionally, ectopic expression of DUSP12 using a

© 2019 The Authors. Hepatology published by Wiley Periodicals, Inc., on behalf of American Association for the Study of Liver Diseases. This is an open access article under the terms of the Creative Commons Attribution-NonCommercial License, which permits use, distribution and reproduction in any medium, provided the original work is properly cited and is not used for commercial purposes.

View this article online at wileyonlinelibrary.com.
DOI 10.1002/hep.30597

Potential conflict of interest: Nothing to report.

ARTICLE INFORMATION:

From the [1]Cardiovascular Hospital, the First Affiliated Hospital of Zhengzhou University, Zhengzhou University, Zhengzhou, China; [2]Department of Endocrinology, the First Affiliated Hospital of Zhengzhou University, Zhengzhou University, Zhengzhou, China; [3]Cardiovascular Research Center, Department of Physiology, Lewis Katz School of Medicine, Temple University, Philadelphia, PA; [4]Gastroenterology Hospital, the First Affiliated Hospital of Zhengzhou University, Zhengzhou University, Zhengzhou, China; [5]Department of Rheumatology and Immunology, the First Affiliated Hospital of Zhengzhou University, Zhengzhou University, Zhengzhou, China.

ADDRESS CORRESPONDENCE AND REPRINT REQUESTS TO:

Yan-Zhou Zhang, M.D., Ph.D.
E-mail: zhangyanzhou2050@sina.com
Tel.: 0371-67967662
or
Jian-Zeng Dong, M.D., Ph.D.
E-mail: jz_dong@126.com
Tel.: 0371-67967662
or
Ling Li, M.D., Ph.D.
Cardiovascular Hospital, the First Affiliated Hospital of Zhengzhou University, Zhengzhou University
No. 1 Jianshe East Road
Zhengzhou, Henan 450052, China
E-mail: liling63035@sina.com
Tel.: 0371-67967662

retroviral expression system induced the suppression of adipogenic differentiation and lipid accumulation.[17] More recently, studies showed that DUSP12 could protect against microbial infection by inhibiting MAPK-mediated expression of proinflammatory mediators such as tumor necrosis factor alpha (TNF-α), interleukin (IL)-1β, and monocyte chemoattractant protein 1.[18] Providing further support, DUSP12 deficiency apparently aggravated pressure overload–induced cardiac hypertrophy and fibrosis by inhibiting activation of JUN N-terminal kinase (JNK).[19] However, the function of DUSP12 in hepatic steatosis and NAFLD is still unknown. Based on the roles of DUSP12 in lipid accumulation, inflammation, and fibrosis and the ability of DUSP12 to regulate MAPK signaling, which is well known in the pathogenesis of NAFLD, we hypothesize that DUSP12 may play an important role in the pathogenesis of NAFLD.

In this study, we revealed that DUSP12 expression was remarkably decreased in the livers of mice fed a high-fat diet (HFD). We demonstrate that hepatocyte-specific DUSP12-deficient (DUSP12-CKO) mice exhibit hepatic steatosis, IR, and inflammation, whereas DUSP12-transgenic (DUSP12-TG) mice protected against HFD-induced steatosis and show improved insulin sensitivity. Moreover, DUSP12 also serves as a master regulator in NAFLD by regulating apoptosis signal–regulating kinase 1 (ASK1) phosphorylation. Finally, our findings suggest that DUSP12 is a potential therapeutic target for lipid metabolism disorders.

Materials and Methods

ANIMAL LIVER SAMPLES

Adult male mice (C57BL/6) aged 8-10 weeks (19-29 g) were housed at 25 ± 5°C under a 12-hour light/dark cycle with free access to water and food. The mice were fed an HFD (60.9% fat, 21.8% carbohydrate, and 18.3% protein; D12492; Research Diets) for 24 weeks and a high-fat high-cholesterol (HFHC) diet (42% fat, 44% carbohydrate, 14% protein, and 0.2% cholesterol; TP26304; Trophic Diets, Nantong, China) for 16 weeks. A normal chow (NC) diet (4% fat, 78% carbohydrate, and 18% protein; D12450J; Research Diets) was used as a control. Ob/Ob mice were fed an NC diet for 8 weeks.

CELL LINES

The human normal hepatocyte cell line L02 and HEK293T cells were purchased from the Type Culture Collection of the Chinese Academy of Sciences (Shanghai, China). All cell lines in our laboratory were passaged no more than 30 times after resuscitation and were routinely tested for mycoplasma contamination using PCR. The cells were cultured in standard medium comprising Dulbecco's modified Eagle's medium, 10% fetal bovine serum, and 1% penicillin–streptomycin and maintained in a humidified 5% CO_2 atmosphere in a cell incubator at 37°C.

WESTERN BLOTTING ANALYSIS

A total of 40-50 μg of protein was subjected to a 10% sodium dodecyl sulfate–polyacrylamide gel electrophoresis gel, transferred to a polyvinylidene difluoride membrane, and incubated with corresponding primary antibodies overnight at 4°C. The indicated antibodies are listed in Supporting Table S1.

LENTIVIRUS VECTOR CONSTRUCTION

Overexpression and knockdown plasmids were obtained to construct lenti-DUSP12 and shDUSP12 virus, and green fluorescent protein and shRNA were used as controls. A kinase inactive mutant plasmid was obtained to construct lenti-dominant negative ASK1 viruses as described.[20] The lentiviruses were packaged using Opti-MEM reduced serum medium, pMD2.G, and overexpression plasmids, as well as polyethylenimine, and then used to infect 293T cells. Lentivirus supernatant was collected 48 hours later and used to infect L02 cells along with polybrene; then, the cells were selected with puromycin.

IN VITRO CELL MODEL OF LIPID ACCUMULATION

Palmitic acid (PA) powder (P0500; Sigma-Aldrich) was dissolved in 0.01 M NaOH to make a stock solution. The PA stock solution was diluted by mixing the indicated culture medium with 25% bovine serum albumin (BSA; BAH66-0050; Equitech-Bio) to make a PA solution. Oleic acid (OA; O1008; Sigma) was

dissolved in 0.01 M NaOH to the indicated concentration. For oil red O staining assays, PA and OA stock solutions with 25% BSA were mixed and diluted with medium to the final concentrations of PA/OA (0.5 mM/1 mM). The cells were then stained with 60% oil red O (O1391; Sigma) working solution for 10 minutes to examine the level of lipid accumulation. Intracellular triglyceride levels were measured using the commercially available Triglyceride Colorimetric Assay Kit (10010303; Cayman) according to the manufacturer's protocol.

IMMUNOFLUORESCENCE STAINING

Paraffin sections were labeled with primary antibodies (ab75476, 1:100; Abcam) overnight, followed by incubation with secondary antibody for 1 hour. Immunofluorescence images were obtained using a fluorescence microscope with DP2-BSW software.

MICE

DUSP12-CKO mice were obtained using clustered regularly interspaced short palindromic repeats (CRISPR)/CRISPR-associated 9 methods. The second and third exons were flanked by loxP sites, and two single-guide RNAs (sgRNA1 and sgRNA2) targeting introns 1 and 3 were thus designed. The donor vector contained exons 2 and 3 flanked by two loxP sites. The PCR primers P1 to P5 used for identification are listed in Supporting Table S2. All products were confirmed by sequencing. Full-length mouse DUSP12 complementary DNA was cloned downstream of the albumin promoter. Hepatocyte-specific DUSP12-TG mice were then produced by microinjecting the albumin–DUSP12 construct into fertilized mouse embryos (C57BL/6 background). Transgenic mice were identified by PCR analysis of tail genomic DNA. Primers were designed for DUSP12 identification as follows: 5′-GGAACAGCTCCAGATGGCAA-3′ and 5′-GCGACTGACTCCTGCATGAC-3′.

MOUSE EXPERIMENTS

Mouse body weight, fasting blood glucose levels, and fasting serum insulin levels were determined at different time points during the experiments. Fasting blood glucose and fasting serum insulin levels were assessed using a glucometer and enzyme-linked immunosorbent assays, respectively, after the mice were fasted for 6 hours. For glucose tolerance tests (GTTs), mice were injected intraperitoneally with 1 g/kg glucose after a 6-hour fast, whereas for insulin tolerance tests (ITTs), 0.75 U/kg insulin was injected intraperitoneally after a 6-hour fast. Blood glucose concentrations in tail blood samples were detected using a glucometer at baseline and at 15, 30, 60, and 120 minutes after injection.

HISTOLOGICAL ANALYSIS

Liver sections were embedded in paraffin and stained with hematoxylin and eosin (H&E) to visualize the morphology of the cells in the tissues. Oil red O staining of frozen liver sections was used to assess lipid droplet accumulation. Images were acquired with a light microscope (Olympus, Tokyo, Japan). Liver fibrosis was assessed by picrosirius red (26357-02; Hede Biotechnology Co., Ltd.) staining. A digital image analysis system (Image-Pro Plus, version 6.0) was used to examine the cross-sectional images of the fibrotic areas.

QUANTITATIVE RT-PCR

RT-PCR was performed with SYBR Green. mRNA levels were normalized to the corresponding β-actin expression levels. The primers used in this study are presented in Supporting Table S3.

MOUSE HEPATIC LIPID ANALYSES

Triglyceride, total cholesterol (TC), and nonesterified fatty acid (NEFA) levels were measured using commercial kits (290-63701 for triglyceride assay, 294-65801 for TC assay, 294-63601 for NEFA assay; Wako, Osaka, Japan).

LIVER FUNCTION ASSAY

Liver function was evaluated in the animals by determining serum alanine aminotransferase (ALT) and aspartate aminotransferase (AST) concentrations using an ADVIA 2400 Chemistry System analyzer (Siemens, Tarrytown, NY) according to the manufacturer's instructions.

PLASMID CONSTRUCTS

Full-length sequences for the human DUSP12 coding region were subcloned into pcDNA5-Flag and phage-Flag vectors to generate the pcDNA5-Flag-DUSP12 and phage-Flag-DUSP12 recombinant plasmids. The DUSP12 and ASK1 coding region were cloned into a vector containing glutathione *S*-transferase (GST)-HA to obtain GST-HA-DUSP12 and GST-HA-ASK1. DUSP12 truncations (1-169, 1-298, and 170-340 amino acids) were obtained by PCR amplification. The products of the DUSP12 residues were digested with the corresponding enzyme and ligated into pcDNA5-Flag to obtain the corresponding plasmids. Similarly, pcDNA5-HA-ASK1, pcDNA5-Flag-ASK1, and HA-labeled ASK1 truncations (1-678, 1-384, 385-678, 679-936, and 937-1374 amino acids) were constructed. The primers used to generate these constructs are listed in Supporting Table S4.

IMMUNOPRECIPITATION

HEK293T cells were cotransfected with the indicated plasmids, and cell lysates were precleared with protein A/G-agarose beads and incubated overnight at 4°C with the indicated antibody. Immunoprecipitated (IP) proteins were identified by immunoblotting.

GST PRECIPITATION ASSAYS

The direct interaction between DUSP12 and ASK1 was determined using GST precipitation assays. Briefly, Rosetta (DE3) *Escherichia coli* cells were transformed with the vector pGEX-4T-1-GST-DUSP12 or pGEX-4T-1-GST-ASK1, and expression was induced using 0.5 mM isopropyl β-D-thiogalactopyranoside. The *E. coli* were lysed, and the extracts were incubated with glutathione–Sepharose 4B beads at 4°C for 1 hour. The beads were then incubated with purified Flag-tagged ASK1, which was prepared through IP, for an additional 4 hours. Proteins that interacted were eluted with elution buffer (50 mM Tris-HCl [pH 8.0] and 20 mM reduced glutathione) and subjected to immunoblotting using anti-Flag antibodies. Extracts from *E. coli* expressing only a GST tag were used as the negative control.

STATISTICAL ANALYSIS

Unless otherwise noted, all data are presented as the means ± SEM. Statistical analysis of data with more than two groups was evaluated by one-way analysis of variance. Data from two groups were analyzed by two-tailed Student *t* test. $P < 0.05$ was defined as statistically significant.

ADDITIONAL METHODS

Detailed methods are provided in the Supporting Information.

Results

DUSP12 EXPRESSION IS DOWN-REGULATED IN FATTY LIVER

To examine the association between DUSP12 and fatty liver, we first evaluated the expression of DUSP12 in obese mice. Eight-week-old mice were fed an HFD or NC for 24 weeks. The protein expression of DUSP12 in the liver was down-regulated in HFD mice compared with control mice (Fig. 1A). As expected, DUSP12 was also decreased in the liver of Ob/Ob mice compared with lean mice (Fig. 1B). These data were further confirmed in the cultured normal human hepatocyte cell line L02 treated with 1% BSA or 0.5 mM PA and 1.0 mM OA for 24 hours. DUSP12 protein expression was down-regulated in PA/OA-treated L02 cells (Fig. 1C). However, the mRNA level of DUSP12 was not changed either *in vivo* or *in vitro*, indicating a posttranslational modification of DUSP12 (Supporting Fig. S1). These results indicate that DUSP12 could play an important role in the pathogenesis of hepatic steatosis.

DUSP12 INHIBITS LIPID ACCUMULATION AND INFLAMMATION AFTER PA/OA TREATMENT *IN VITRO*

The down-regulation of DUSP12 expression in fatty liver prompted us to investigate the functional role of DUSP12 in lipid metabolism. DUSP12 was knocked down in L02 cells using siRNAs (Fig. 2A,B). Treatment with PA/OA further increased the number of lipid droplets in cells expressing low levels of DUSP12 compared with the control cells (Fig. 2C). Triglyceride levels were also significantly higher in the siDUSP12 groups (Fig. 2D). The mRNA levels of acetyl-coenzyme A carboxylase alpha (ACACα), fatty

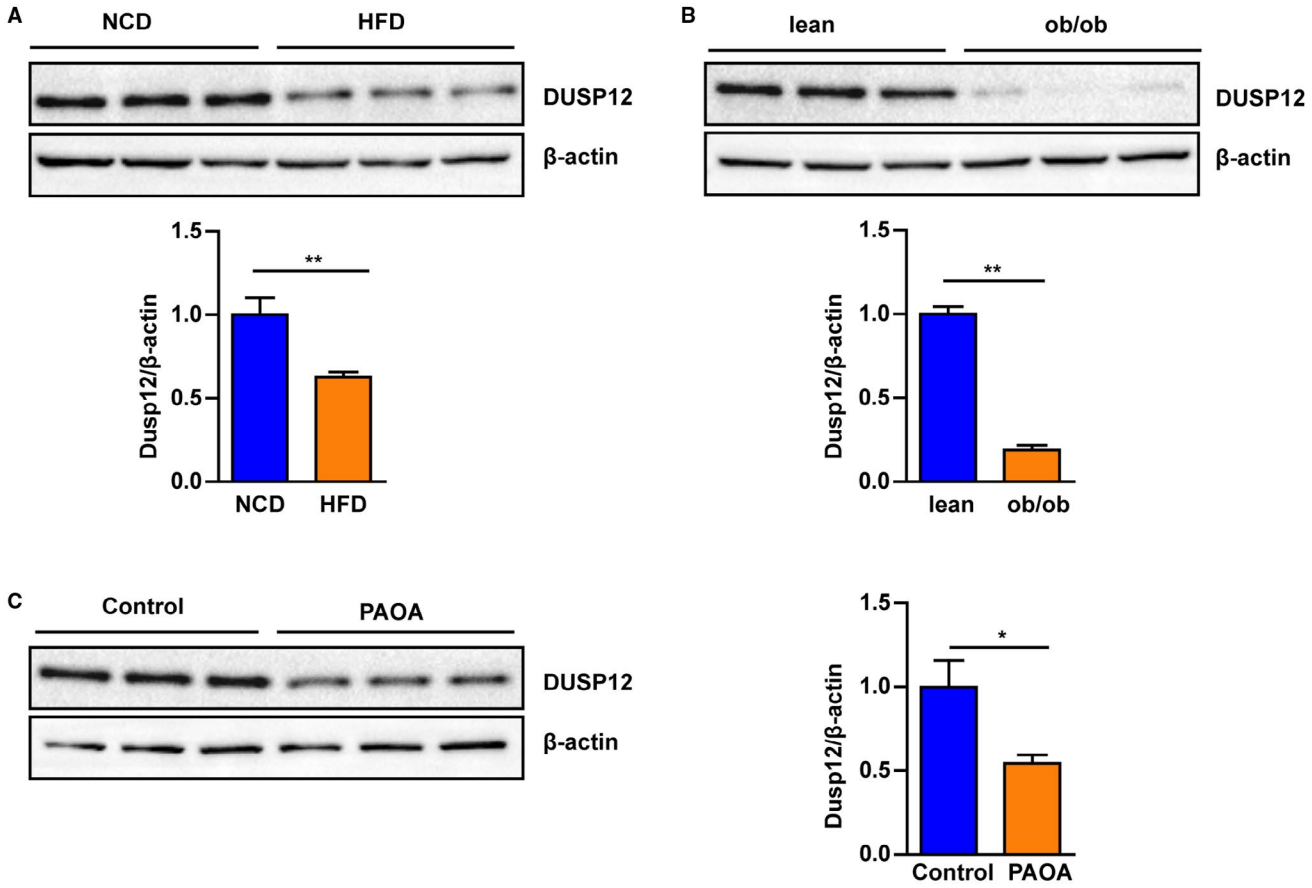

FIG. 1. DUSP12 expression in the liver and in L02 cells. (A) Representative western blot of DUSP12 expression in liver samples of C57BL/6J mice that were fed an HFD or NC for 24 weeks (n = 6/group). (B) Representative protein expression of DUSP12 in the livers of lean and ob/ob mice (n = 6/group). (C) Protein expression of DUSP12 in the normal human hepatocyte cell line L02 treated with PA/OA (0.5/1.0 mM; n = 3 independent experiments). Quantification of protein expression levels was normalized to β-actin levels. Data are expressed as the mean ± SEM. **P* < 0.05, ***P* < 0.01.

acid synthase (FASN), stearoyl-coenzyme A desaturase 1 (SCD-1), and peroxisome proliferator–activated nuclear receptor gamma (PPARγ) were then examined. The results showed that ACACα, FASN, SCD, and PPARγ mRNA expression was increased significantly in siDUSP12-transfected cells compared with control cells after treatment with PA/OA (Fig. 2E). Additionally, the expression levels of IL-6 and TNF-α were increased in PA/OA-treated, siDUSP12-transfected cells compared to controls (Fig. 2F).

Next, we investigated whether overexpression of DUSP12 could have an opposite effect on lipid metabolism and inflammation (Supporting Fig. S2A). The number of lipid droplets and triglyceride levels sharply decreased in cells overexpressing DUSP12 compared with cells expressing the lentiviral vector alone upon treatment with PA/OA (Supporting Fig. S2B,C). Moreover, the mRNA levels of ACACα, FASN, SCD, and PPARγ were decreased significantly in the DUSP12-overexpressing cells (Supporting Fig. S2D). Consistently, IL-6 and TNFα expression were also decreased in the DUSP12-overexpressing cells (Supporting Fig. S2E). Taken together, these results demonstrate that DUSP12 protects against lipid accumulation and inflammation after PA/OA stimulation.

DEFICIENCY OF DUSP12 TRIGGERS HEPATIC STEATOSIS

To clarify the effect of DUSP12 on hepatic steatosis *in vivo*, we established DUSP12-CKO mice

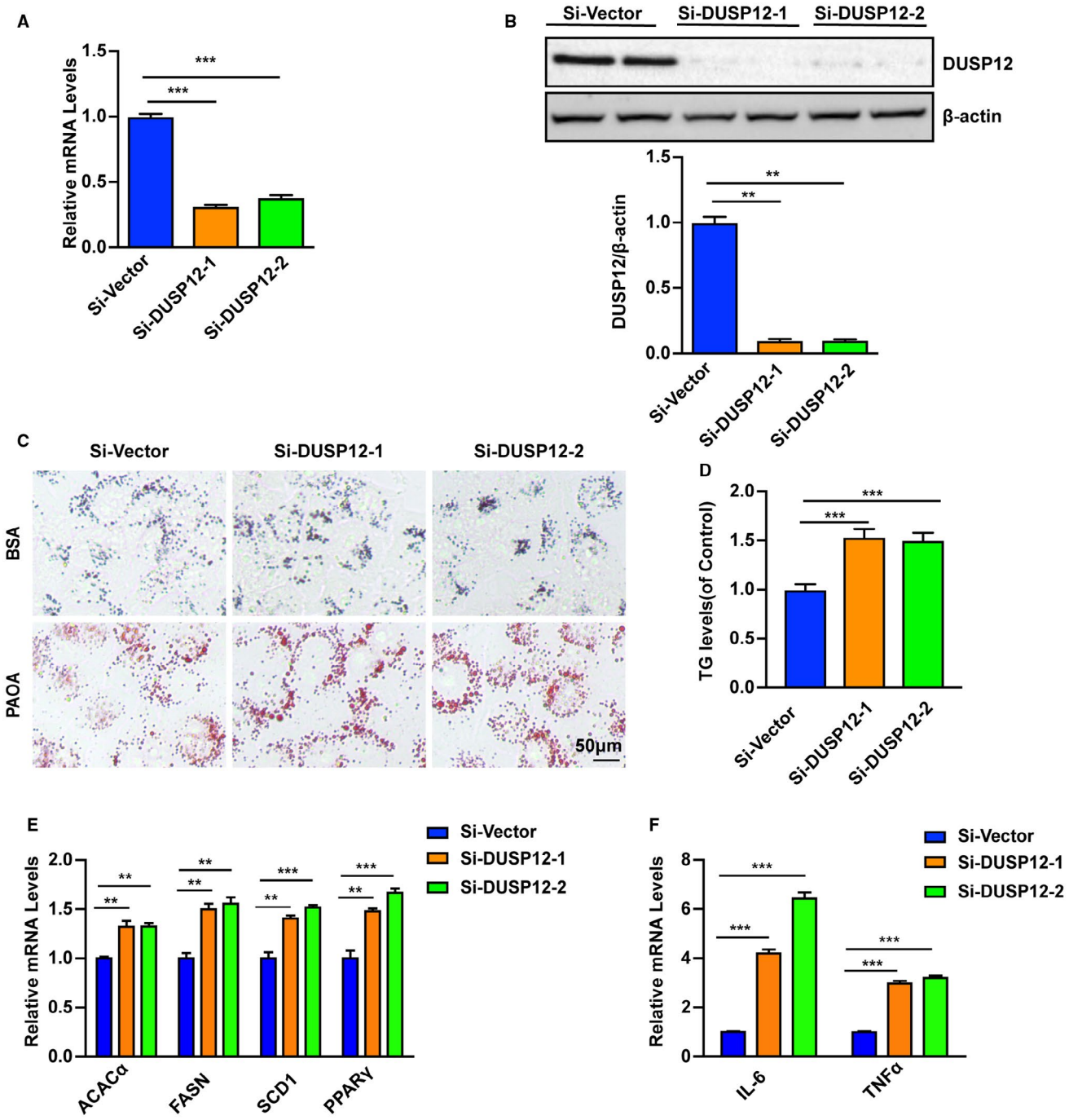

FIG. 2. DUSP12 reduces PA/OA-induced lipogenesis and inflammation in L02 cells. (A) Relative mRNA levels of DUSP12 were determined by real-time quantitative PCR. (B) DUSP12 protein expression levels were evaluated by western blotting. n = 3 independent experiments. (C) Representative oil red O staining and (D) relative intracellular triglyceride levels of L02 cells transfected with different siRNAs after treatment with PA/OA (0.5/1.0 mM), n = 3 independent experiments; bar, 50 μm. (E) Relative mRNA levels of lipid metabolism–related genes and (F) proinflammatory markers in L02 cells transfected with different siRNAs after treatment with PA/OA, n = 3 independent experiments. Data represent the mean ± SEM. $^{**}P < 0.01$, $^{***}P < 0.001$. Abbreviation: TG, triglyceride.

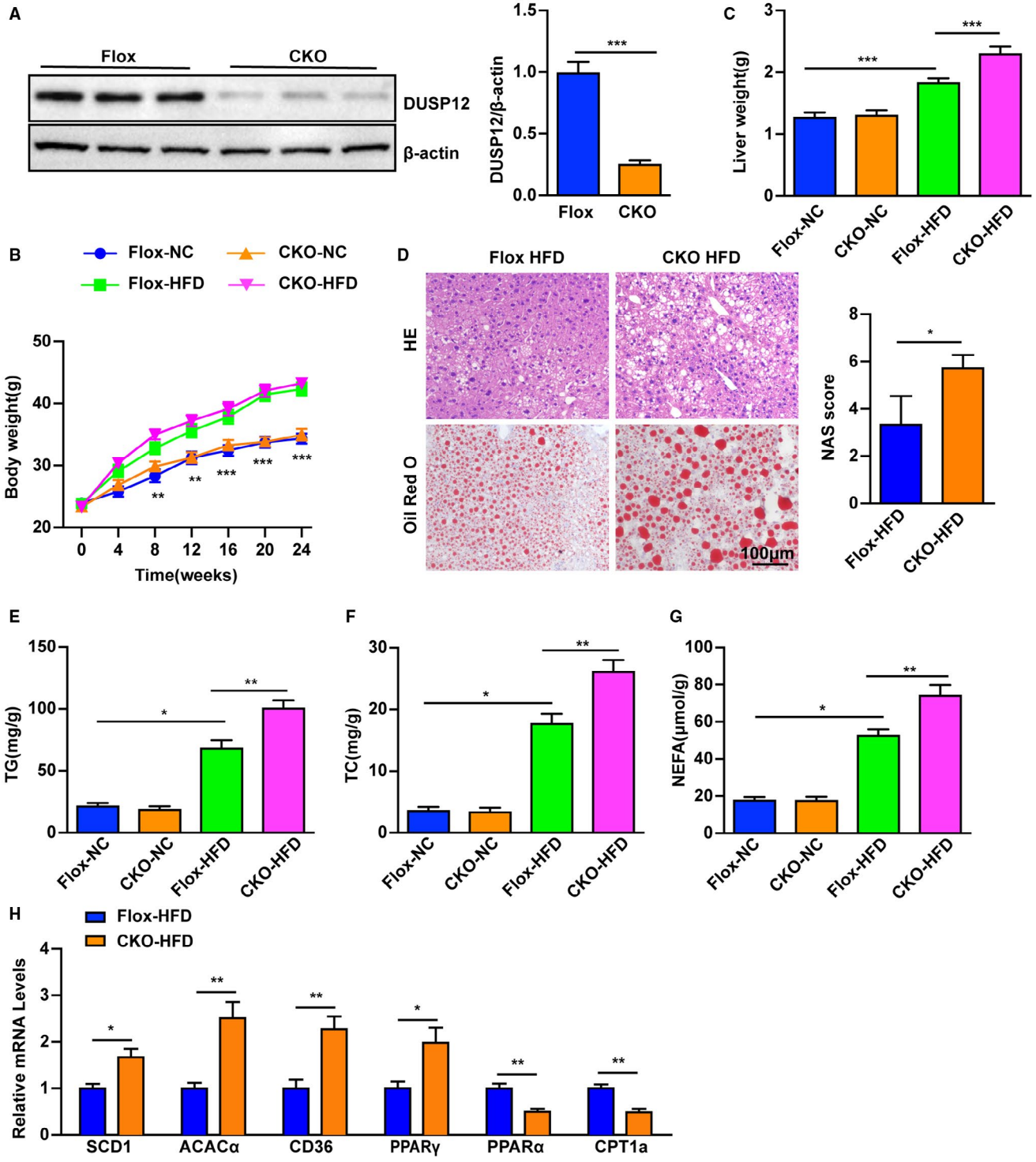

(Supporting Fig. S3A-C; Fig. 3A). Subsequently, DUSP12-CKO and littermate Flox mice were fed an HFD for 24 weeks. The results showed that, compared to control mice, DUSP12-CKO mice showed no significant difference in body weight but had a higher liver weight after consuming an HFD for 24 weeks (Fig. 3B,C). Liver sections stained with H&E and oil red O showed that the DUSP12-CKO

FIG. 3. Deficiency of DUSP12 aggravates hepatic steatosis. (A) Representative blot of DUSP12 expression in liver samples from DUSP12-Flox and DUSP12-CKO mice (n = 3). (B) Body weight and (C) liver weight of DUSP12-CKO mice and their littermate controls fed for 24 weeks with NC or an HFD (n = 10). For (B), $^{**}P < 0.01$, $^{***}P < 0.001$ Flox-HFD versus Flox-NC group. (D) Images of H&E and oil red O staining of liver tissues from Flox and DUSP12-CKO mice fed an HFD for 24 weeks (n = 6/group). Scale bar, 100 μm. NAFLD activity score of the Flox and DUSP12-CKO mice fed an HFD for 24 weeks (n = 6 for each group). (E) Triglyceride, (F) TC, and (G) NEFA levels in the livers of Flox and DUSP12-CKO mice at the end of 24 weeks of HFD feeding (n = 10 mice for each group). (H) Relative mRNA levels of lipid metabolic genes, including lipogenesis genes and oxidation-related genes, in Flox and DUSP12-CKO mice fed an HFD for 24 weeks (n = 4/group). The mRNA and protein expression levels of the genes were normalized to that of β-actin. Data represent the mean ± SEM. $^{*}P < 0.05$, $^{**}P < 0.01$, $^{***}P < 0.001$. Abbreviations: NAS, NAFLD activity score; TG, triglyceride.

mice fed an HFD exhibited a remarkable increase in lipid accumulation compared to control littermate mice (Fig. 3D). DUSP12-CKO mice fed an HFD also showed increased levels of triglyceride, TC, and NEFA in the liver compared to controls (Fig. 3E-G). Furthermore, the mRNA levels of lipid metabolic genes, including the fatty acid synthesis genes SCD1, ACACα, and PPARγ and the fatty acid uptake gene cluster of differentiation 36 (CD36) were significantly increased in the liver of DUSP12-CKO mice, whereas the fatty acid β-oxidation genes PPARα and carnitine palmitoyltransferase 1a (CPT1a) were decreased (Fig. 3H). These data suggest that DUSP12 deficiency may contribute to HFD-induced hepatic steatosis.

DUSP12 DEFICIENCY EXACERBATES HFD-INDUCED HEPATIC INSULIN RESISTANCE AND INFLAMMATION

Next, we examined whether DUSP12 deficiency could exacerbate HFD-induced insulin resistance. DUSP12-CKO mice fed an HFD had consistently increased fasting glucose levels compared with their DUSP12-Flox counterparts (Fig. 4A). Additionally, glucose tolerance was increased and insulin sensitivity was compromised in the DUSP12-CKO mice compared with the DUSP12-Flox mice, as shown by the GTTs and ITTs, respectively (Fig. 4B,C). Plasma insulin levels were increased in DUSP12-CKO mice compared with their counterparts at the end of 24 weeks of HFD feeding (Fig. 4D). The mRNA levels of genes related to gluconeogenesis, phosphoenolpyruvate carboxykinase (PCK1) and glucose-6-phosphatase (G6PC), were also significantly higher in DUSP12-CKO mice (Fig. 4E).

Because inappropriate NF-κB pathway activation and inflammation increase the likelihood of hepatic steatosis progression to cirrhosis and liver damage,[21] we examined whether NF-κB signaling is regulated by DUSP12 during HFD-induced hepatic steatosis. Activation of inhibitor of kappa light polypeptide gene enhancer in B cells (IKBα) was significantly decreased, while phosphorylation levels of IKKβ and P65 were significantly enhanced in DUSP12-CKO mice compared with DUSP12-Flox mice (Fig. 4F). Moreover, the mRNA levels of proinflammatory cytokines (TNF-α, IL-6) and chemokine (C-C motif) ligand 2 (CCL2) were significantly higher, while the anti-inflammatory cytokine IL-10 was significantly lower in DUSP12-CKO mice (Fig. 4G). Quantification of serum ALT and AST levels in mice confirmed that DUSP12-CKO mice were sensitive to HFD-induced liver injury (Fig. 4H,I). Collectively, these data revealed that DUSP12 deficiency promotes IR and inflammation after HFD treatment.

DUSP12 OVEREXPRESSION REDUCES HFD-INDUCED HEPATIC STEATOSIS, IR, AND INFLAMMATION

To determine whether DUSP12 overexpression could reduce HFD-induced hepatic steatosis, we also generated hepatocyte-specific DUSP12-TG mice (Supporting Fig. S4A). Body weight showed no significant change (Supporting Fig. S4B), but liver weight and hepatic lipogenesis were decreased in DUSP12-TG mice fed an HFD compared with DUSP12-NTG controls (Fig. 5A-C). Furthermore, the mRNA levels of SCD1, ACACα, PPARγ, and CD36 were significantly decreased; but the mRNA levels of PPARα and CPT1a were increased in DUSP12-TG mouse liver (Fig. 5D). Fasting blood glucose, GTT, ITT, and fasting insulin levels were also significantly decreased in DUSP12-TG mice compared with their counterparts (Fig. 5E-G; Supporting

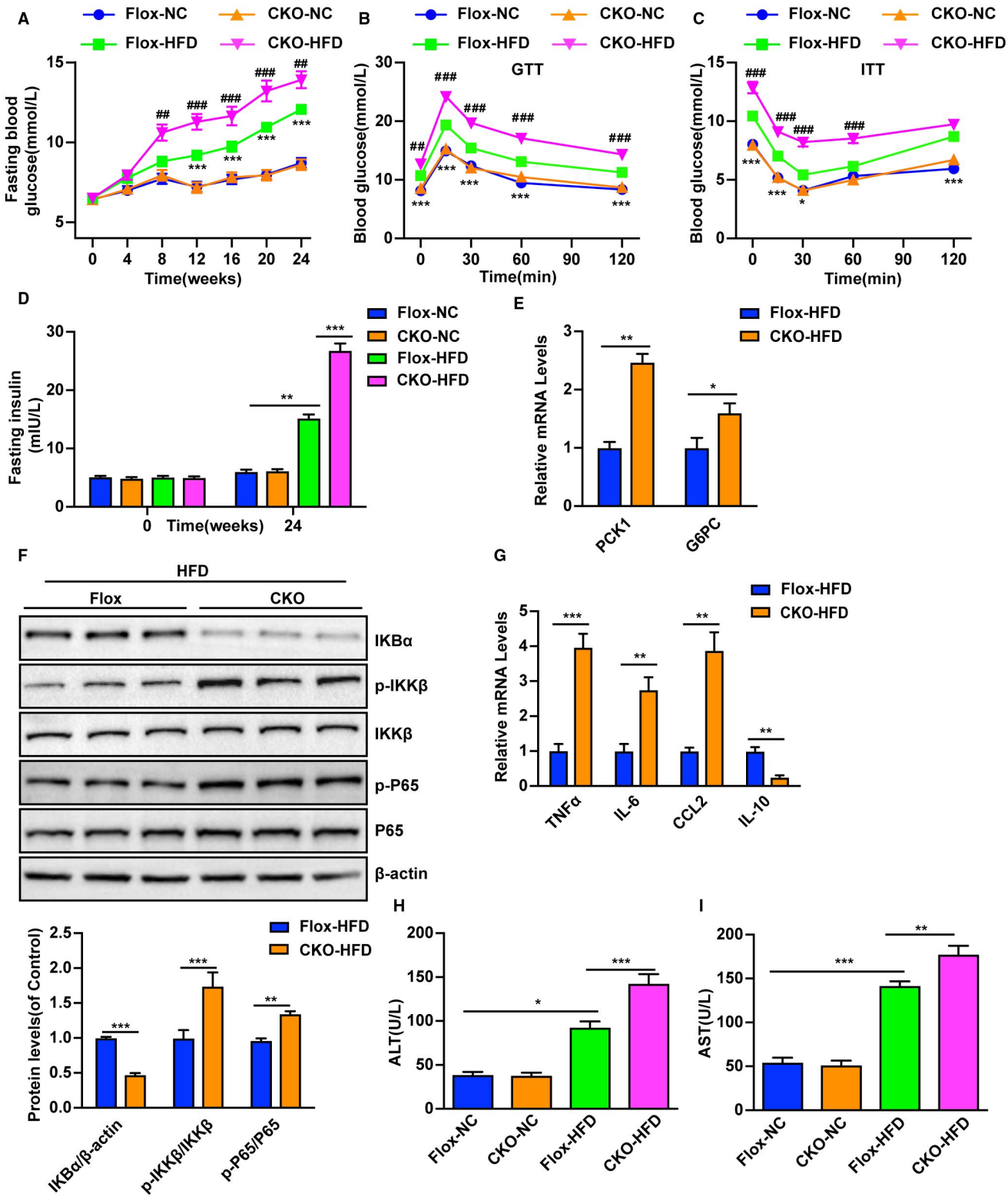
A
Flox-NC
CKO-NC
Flox-HFD
CKO-HFD
Fasting blood glucose(mmol/L)
Time(weeks)
B
GTT
Blood glucose(mmol/L)
Time(min)
C
ITT
Blood glucose(mmol/L)
Time(min)
D
Fasting insulin (mIU/L)
Time(weeks)
E
Relative mRNA Levels
PCK1
G6PC
F
HFD
Flox
CKO
IKBα
p-IKKβ
IKKβ
p-P65
P65
β-actin
Protein levels(of Control)
IKBα/β-actin
p-IKKβ/IKKβ
p-P65/P65
G
Relative mRNA Levels
TNFα
IL-6
CCL2
IL-10
H
ALT(U/L)
I
AST(U/L)

FIG. 4. DUSP12 deficiency exacerbates HFD-induced hepatic insulin resistance and inflammation. (A) Fasting blood glucose levels were measured in DUSP12-Flox and DUSP12-CKO mice fed either NC or an HFD every 4 weeks from 0 to 24 weeks (n = 10/group). (B,C) GTTs (B) and ITTs (C) were performed on DUSP12-CKO and Flox mice after NC or HFD feeding for 22 weeks and 23 weeks, respectively (for each test, n = 10/group). For (A-C), $^{*}P < 0.05$, $^{***}P < 0.001$ indicates DUSP12-Flox-HFD versus DUSP12-Flox-NC; $^{\#\#}P < 0.01$, $^{\#\#\#}P < 0.001$ indicate DUSP12-CKO-HFD versus DUSP12-Flox-HFD. (D) Fasting serum insulin levels were measured in DUSP12-Flox and DUSP12-CKO mice fed either NC or an HFD at 0 and 24 weeks (n = 10/group). (E) Real-time quantitative PCR analysis of the relative mRNA levels of PCK1 and G6PC in the livers of the indicated groups (n = 4/group). (F) Phosphorylated and total levels of IKBα and IKKβ/P65 in liver tissues from HFD-fed DUSP12-KO and DUSP12-Flox mice were determined by western blotting. Target protein expression levels were normalized to the levels of β-actin (n = 6/group). (G) The mRNA levels of proinflammatory cytokines (TNF-α, IL-6), the chemokine CCL2, and the anti-inflammatory cytokine IL-10 were tested by real-time quantitative PCR in DUSP12-KO and DUSP12-Flox mice (n = 4/group). (H) ALT and (I) AST in serum were examined in Flox and DUSP12-CKO mice fed an HFD (n = 10/group). All data represent the mean ± SEM. For D-I, $^{*}P < 0.05$, $^{**}P < 0.01$, $^{***}P < 0.001$.

Fig. S4C). Furthermore, we also examined levels of gluconeogenesis-related genes, PCK1 and G6PC, which were significantly decreased in DUSP12-TG mouse liver (Supporting Fig. S4D). Phosphorylation of IKBα was significantly increased, while phosphorylation levels of IKKβ and P65 were significantly decreased in DUSP12-TG compared with nontransgenic (NTG) mice fed an HFD (Fig. 5H). Furthermore, the mRNA levels of TNF-α, IL-6, and CCL2 were also significantly lower, while IL-10 mRNA levels were higher in DUSP12-TG mice fed an HFD than in DUSP12-NTG mice (Fig. 5I). Similarly, our data showed that serum levels of ALT and AST were significantly decreased in DUSP12-TG mice fed an HFD compared with NTG mice (Supporting Fig. S4E,F). These data suggest a protective effect of DUSP12-TG on mice with HFD-induced hepatic steatosis.

DUSP12 DEFICIENCY AGGRAVATES HFHC DIET–INDUCED LIVER FIBROSIS AND INFLAMMATION

To determine whether DUSP12 deficiency could promote liver inflammation and fibrosis in NASH, we established a NASH model using an HFHC diet in mice.[22] Like the HFD-induced response, body weight was similar, while liver weight was significantly increased in DUSP12-CKO mice compared with control mice (Fig. 6A,B). Hepatic lipid accumulation (Fig. 6C) and triglyceride and TC levels (Fig. 6D,E) were also significantly higher in DUSP12-CKO mice. Consistent with this finding, the mRNA levels of genes involved in fatty acid synthesis, such as SCD1, CD36, and PPARγ, were all significantly greater in DUSP12-CKO mouse liver than in control mouse liver, while PPARα significantly decreased (Fig. 6F). Moreover, the DUSP12-CKO mice showed higher fasting blood glucose (Fig. 6G) and impaired glucose resistance (Fig. 6H) and insulin sensitivity (Fig. 6I). In addition, immunofluorescence staining showed that the number of inflammatory cells infiltrating the liver of DUSP12-CKO mice was significantly greater than that of the control group (Fig. 6J). These findings were further corroborated by data showing higher mRNA levels of inflammatory markers and lower mRNA levels of anti-inflammatory markers in DUSP12-CKO mice fed an HFHC diet compared to controls (Fig. 6K). Notably, collagen deposition and mRNA levels of profibrotic genes were all significantly greater in the liver of DUSP12-CKO mice than in the liver of control mice fed an HFHC diet (Fig. 6L,M). These data show that DUSP12 deficiency is responsible for HFHC-induced liver inflammation and fibrosis.

DUSP12 REGULATES p38 AND JNK SIGNALING PATHWAYS THROUGH ASK1 PHOSPHORYLATION

Subsequently, we investigated the mechanisms by which DUSP12 inhibits the progression of NAFLD/NASH. Considering that DUSP12 could regulate microbial infection and cardiac hypertrophy through modulating MAPK signaling,[18] MAPK pathways are well known to regulate metabolic dysfunction and hepatic steatosis during the pathogenesis of NAFLD.[23] Thus, we examined whether DUSP12 could regulate MAPK signaling in hepatic steatosis. Phosphorylation of JNK and p38 was increased in liver samples of DUSP12-CKO mice compared with DUSP12-Flox mice fed an HFD (Supporting Fig. S5A). In contrast, phosphorylation of JNK and p38 was decreased in DUSP12-TG mice compared with DUSP12-NTG mice (Supporting Fig. S5B).

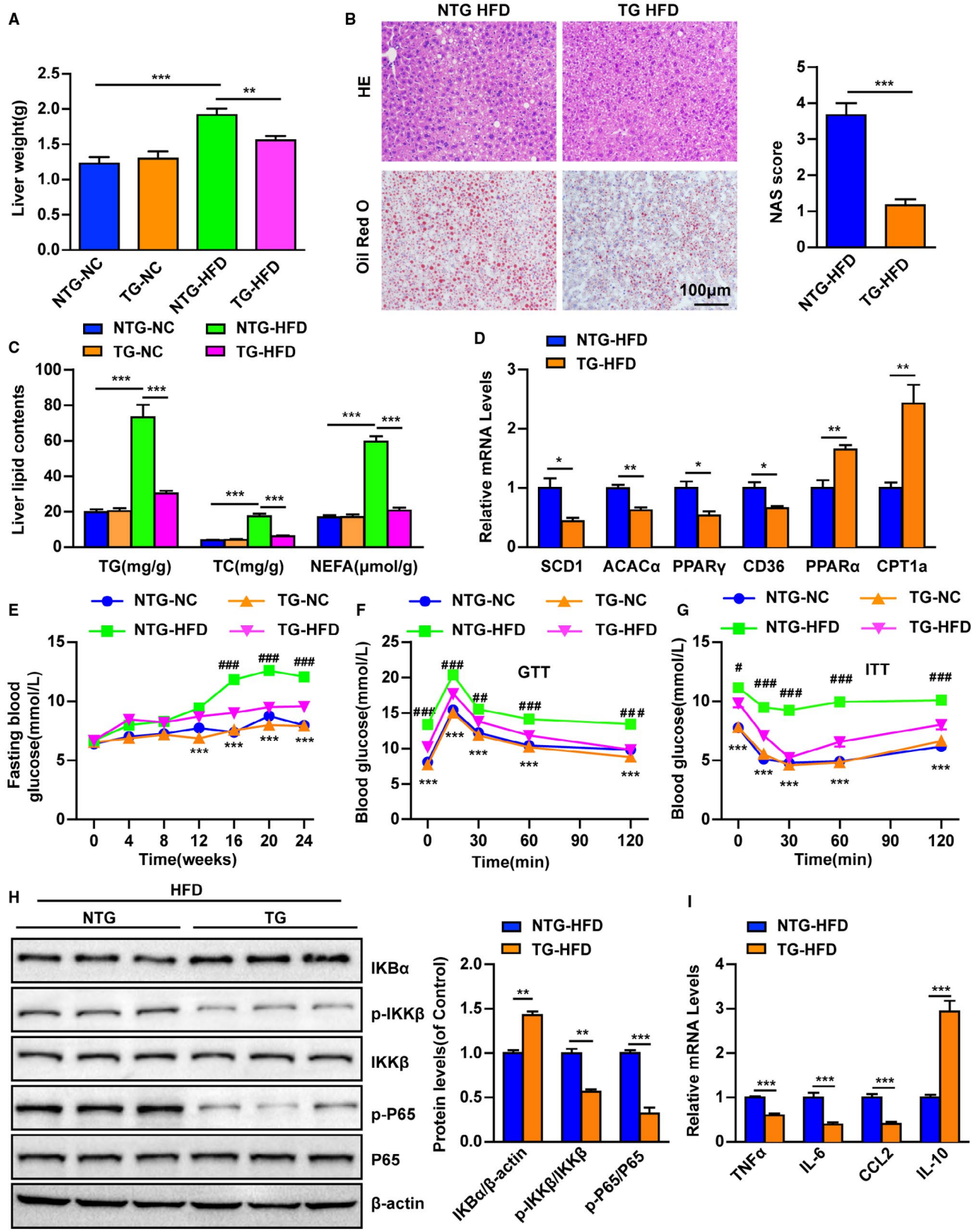
A
Liver weight(g)
NTG-NC
TG-NC
NTG-HFD
TG-HFD
B
NTG HFD
TG HFD
HE
Oil Red O
100μm
NAS score
C
Liver lipid contents
TG(mg/g)
TC(mg/g)
NEFA(μmol/g)
D
Relative mRNA Levels
SCD1
ACACα
PPARγ
CD36
PPARα
CPT1a
E
Fasting blood glucose(mmol/L)
Time(weeks)
F
GTT
Blood glucose(mmol/L)
Time(min)
G
ITT
Blood glucose(mmol/L)
Time(min)
H
HFD
NTG
TG
IKBα
p-IKKβ
IKKβ
p-P65
P65
β-actin
Protein levels(of Control)
IKBα/β-actin
p-IKKβ/IKKβ
p-P65/P65
I
Relative mRNA Levels
TNFα
IL-6
CCL2
IL-10

FIG. 5. DUSP12 inhibits HFD-induced lipid content and hepatic glucose metabolism. (A) Liver weight in DUSP12-TG or NTG mice fed an HFD or NC for 24 weeks (n = 10/group). (B) Representative H&E and oil red O staining of liver sections obtained from DUSP12-TG and NTG mice after 24 weeks of HFD feeding (n = 6/group). Scale bar, 100 μm. The NAFLD activity score of DUSP12-TG and NTG mice fed an HFD for 24 weeks (n = 6/group). (C) Triglyceride, TC, and NEFA levels in DUSP12-TG or NTG mice fed an HFD or NC for 24 weeks (n = 10/group). (D) Relative mRNA levels of lipogenesis-related genes were tested by real-time quantitative PCR (n = 4/group). (E) Fasting blood glucose levels were measured in NTG and DUSP12-TG mice fed either NC or an HFD every 4 weeks from 0 to 24 weeks (n = 10/group). (F,G) GTTs (F) and ITTs (G) were performed on DUSP12-TG and NTG mice after NC or HFD feeding for 22 weeks and 23 weeks, respectively (n = 10 in each group). For (E-G), $^{***}P < 0.001$ indicates DUSP12-NTG-HFD versus DUSP12-NTG-NC; $^{\#}P < 0.05$, $^{\#\#}P < 0.01$, $^{\#\#\#}P < 0.001$ indicate DUSP12-TG-HFD versus DUSP12-NTG-HFD. (H) Phosphorylated and total levels of IKBα/IKKβ/P65 in the livers from HFD-fed TG and NTG mice were determined by western blotting. Target protein expression levels were normalized to the levels of β-actin (n = 6/group). (I) Relative mRNA levels of TNF-α, IL-6, CCL2, and IL-10 were examined in DUSP12-TG and DUSP12-NTG mice after HFD feeding (n = 4/group). All data represent the mean ± SEM. For (A-D, H, I), $^{*}P < 0.05$, $^{**}P < 0.01$, $^{***}P < 0.001$. Abbreviations: NAS, NAFLD activity score; TG, triglyceride (C).

However, extracellular signal–regulated kinase phosphorylation was not affected by DUSP12 modulation (Supporting Fig. S5A,B).

To determine possible upstream molecules that mediate the activation of JNK and p38, we examined the activation of several signaling molecules, including TANK-binding kinase (TBK), ASK1, and MAPK kinase 4/7 (MKK4/7). The results showed that phosphorylation of ASK1 and MKK4/7, but not TBK1, was significantly elevated in DUSP12-CKO mice but down-regulated in DUSP12-TG mice (Supporting Fig. S5C,D). Taken together, our findings suggest that the ASK1–MKK4/7–p38/JNK signaling pathway is regulated by DUSP12 during hepatic steatosis and related metabolic disorders.

Next, we investigated how DUSP12 regulates the activation of ASK1. To verify the effect of DUSP12 on ASK1 signaling *in vitro*, we tested the protein expression of Flag-DUSP12 and the phosphorylation of ASK1 signaling pathways, and the results showed that DUSP12 inhibited the phosphorylation of ASK1 signaling pathways after PA/OA treatment (Fig. 7A). We performed a series of IP experiments using the HEK293T cell line. IP experiments demonstrated that DUSP12 coimmunoprecipitated with ASK1 and vice versa (Fig. 7B,C). A GST-tagged DUSP12 efficiently pulled down ASK1 and vice versa (Fig. 7D,E). These results suggest that DUSP12 works directly with ASK1. Next, we created serially truncated forms of DUSP12 and ASK1 and performed co-IP assays to identify which regions of DUSP12 and ASK1 mediate the interaction. The mapping results showed that the domain encompassing amino acids 1-384 on ASK1 bound to the domain encompassing amino acids 1-169 on DUSP12 (Fig. 7F,G).

ASK1 MEDIATED THE EFFECT OF DUSP12 ON HEPATIC STEATOSIS OF LIPID METABOLISM MACHINERY

To further evaluate whether the effect of DUSP12 on the regulation of ASK1 signaling was dependent on its phosphatase activity, we obtained an inactivating mutant containing a point mutation in the catalytic site of DUSP12 (DUSP12-C115S). The results showed that DUSP12-C115S lost its interaction with ASK1 (Fig. 8A) and that DUSP12-C115S showed no inhibitory effect on ASK1 activation (Fig. 8B).

To further address the role of the DUSP12–ASK1 pathway in lipid accumulation, we blocked ASK1 activity in L02 cells expressing either control or DUSP12 short hairpin RNA (Fig. 8C). We found that the hyperactivation of p38 and JNK phosphorylation that resulted from DUSP12 knockdown was inhibited by ASK1 activity inhibition (Fig. 8D). Lipid accumulation potentiated by DUSP12 knockdown was also completely inhibited by ASK1 activity inhibition (Fig. 8E,F). Moreover, blocking ASK1 activity suppressed the up-regulated mRNA expression of lipid metabolism and inflammatory markers in DUSP12 knockdown cells (Fig. 8G,H). These findings present evidence that the DUSP12–ASK1 pathway is directly involved in the regulation of lipid metabolism, which could play a role in hepatic steatosis regulated by DUSP12.

Discussion

NAFLD prevalence has increased, and over the next 10 years NAFLD is expected to be the leading cause

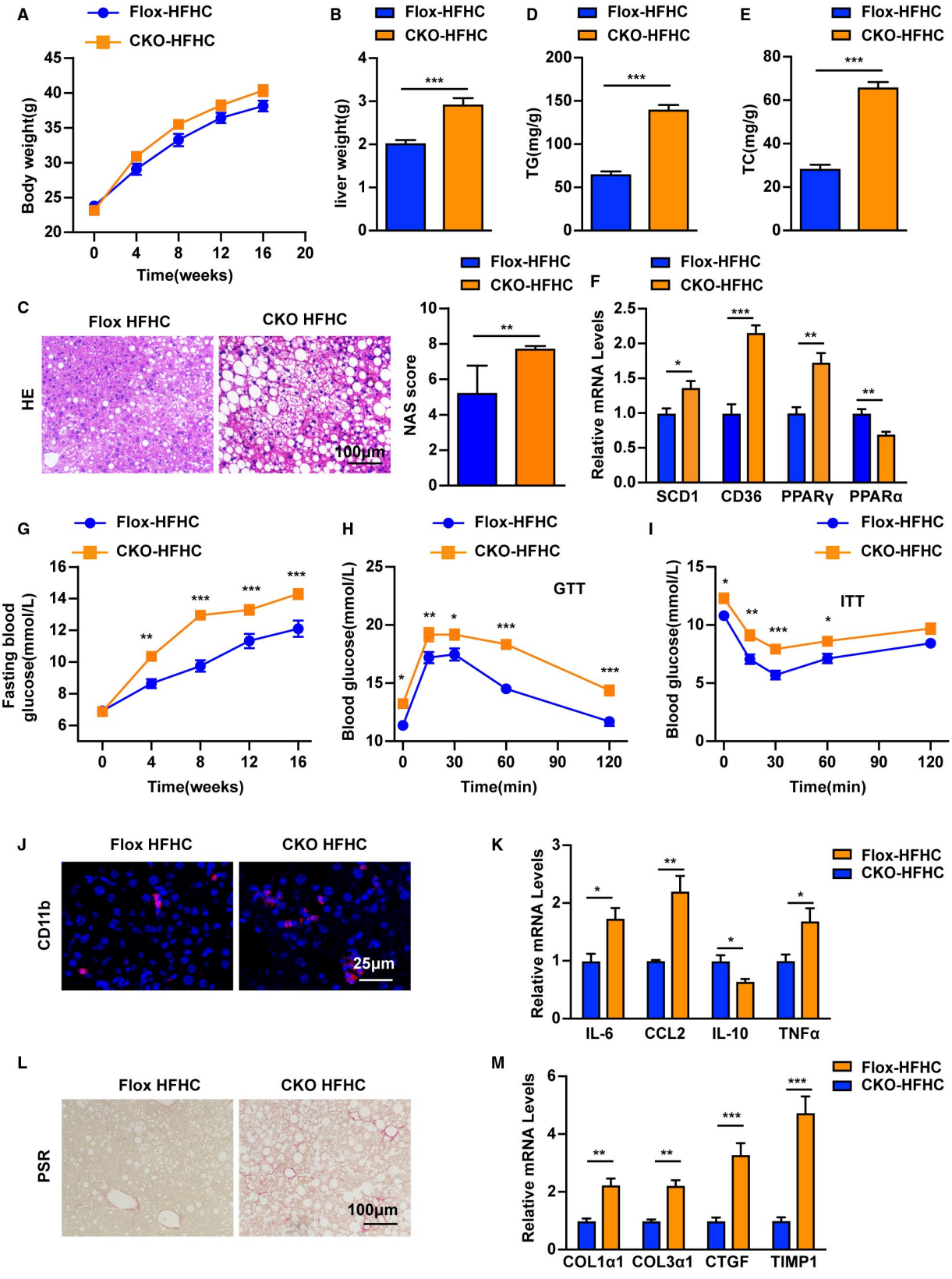
A
Flox-HFHC
CKO-HFHC
Body weight(g)
Time(weeks)
B
liver weight(g)
D
TG(mg/g)
E
TC(mg/g)
C
Flox HFHC
CKO HFHC
HE
100μm
NAS score
F
Relative mRNA Levels
SCD1
CD36
PPARγ
PPARα
G
Fasting blood glucose(mmol/L)
H
GTT
Blood glucose(mmol/L)
Time(min)
I
ITT
J
CD11b
25μm
K
IL-6
CCL2
IL-10
TNFα
L
PSR
100μm
M
COL1α1
COL3α1
CTGF
TIMP1

FIG. 6. DUSP12 deficiency aggravates HFHC-induced liver fibrosis and inflammation. (A) Body weight and (B) liver weight in DUSP12-Flox or DUSP12-CKO mice fed an HFHC for 16 weeks (n = 10/group). (C) Representative H&E staining of liver sections obtained from Flox or DUSP12-CKO mice after 16 weeks of HFHC feeding (n = 6/group). Scale bar, 100 μm. The NAFLD activity score of Flox or DUSP12-CKO mice after 16 weeks of HFHC feeding (n = 6/group). (D) Triglyceride and (E) TC levels in Flox or DUSP12-CKO mice fed an HFHC for 16 weeks (n = 10/group). (F) Relative mRNA levels of lipogenesis-related genes SCD1, CD36, PPARγ, and PPARα were tested by real-time quantitative PCR (n = 4/group). (G) Fasting blood glucose levels were measured in DUSP12-Flox or DUSP12-CKO mice fed an HFHC every 4 weeks from 0 to 16 weeks (n = 10 in each group). (H,I) GTT (H) and ITT (I) were performed on DUSP12-Flox and DUSP12-CKO mice after HFHC feeding for 14 weeks and 15 weeks, respectively (for each test, n = 10/group). (J) Representative images showing immunofluorescence staining for CD11b in the livers of the indicated mice fed an HFHC for 16 weeks. Nuclei were labeled with 4′,6-diamidino-2-phenylindole (blue) (n = 4 mice/group). Scale bar, 25 μm. (K) Relative mRNA levels of cytokines in DUSP12-Flox and DUSP12-CKO mice after HFHC feeding (n = 4 mice/group). (L) Representative picrosirius red staining of liver sections from DUSP12-Flox and DUSP12-CKO mice after HFHC diet for 16 weeks (n = 6 mice/group). (M) mRNA levels of profibrotic genes in livers from mice in the indicated groups (n = 4 mice/group). mRNA expression of target genes was normalized to that of β-actin. All data represent the mean ± SEM. $^{*}P < 0.05$, $^{**}P < 0.01$, $^{***}P < 0.001$. Abbreviations: NAS, NAFLD activity score; PSR, picrosirius red; TG, triglyceride.

of liver pathology in the Western world; NAFLD can progress to liver failure and, consequently, the need for liver transplantation.[24] NAFLD is recognized as the predominant form of chronic liver disease associated with MS, which includes hypertension, type 2 diabetes mellitus (T2DM), obesity, and hyperlipidemia.[25-27] While NAFLD is mostly benign, chronic liver inflammation in NASH may cause progression to fibrosis and hepatocellular carcinoma. Currently, the need for a better understanding of the reasons that drive the progression from NAFLD to NASH and how to use this information both to improve diagnosis and to develop treatment strategies is extremely urgent.[28] Intriguingly, our findings identify a function of DUSP12 in regulating lipid metabolism. DUSP12 deficiency aggravated HFD-induced IR and hepatic steatosis and accelerated HFHC diet–induced inflammatory responses and liver fibrosis. Furthermore, ASK1 activity was essential for DUSP12 deficiency–mediated prevention of HD-induced fatty liver and hepatic steatosis. These observations present evidence that the DUSP12–ASK1 pathway is positively involved in the regulation of NAFLD and NASH and underline DUSP12 as an essential molecular switch regulating lipid metabolism.

DUSP12 is an atypical DUSP that is highly conserved among mammalian species.[29] Recent studies have revealed that DUSP12 acts as a neuroblastoma susceptibility gene, with particular relevance for those at low risk for malignant progression and death from disease.[30] Moreover, DUSP12 could increase the c-met proto-oncogene and the collagen and laminin receptor integrin alpha 1, which is implicated in metastasis.[29] While an increasing number of studies have focused on the role of DUSP12 in regulating multiple critical signaling pathways, the potential role of DUSP12 in the liver, especially in NAFLD, remains uncharacterized. In contrast, our study using DUSP12-CKO mice revealed a hepatic steatosis resistance phenotype under HFD conditions. Furthermore, DUSP12-CKO mice fed an HFD also showed an increase in liver weight as well as increased triglyceride, TC, and NEFA levels. Additionally, DUSP12 deficiency exacerbates HFD-induced hepatic IR and inflammation. Further study on the correlations between DUSP12 and hepatic steatosis may provide guidance for the treatment of certain types of metabolic disease.

NAFLD is characterized by an accumulation of intrahepatic lipids. Lipotoxicity is emerging when the hepatic capability to use, store, and output free fatty acids as triglycerides is surpassed by free fatty acid flux or liver *de novo* lipogenesis,[31] thus triggering hepatocyte death, inflammation, and fibrosis.[32] Interestingly, our study demonstrates that the liver sections of DUSP12-CKO mice fed an HFD exhibited a remarkable increase in lipid accumulation as evidenced by staining with H&E and oil red O. Consistently, the mRNA levels of lipid metabolic genes, including the fatty acid synthesis genes SCD1, ACACα, and PPARγ and the fatty acid uptake gene CD36, were significantly increased in the liver of DUSP12-CKO mice, whereas the fatty acid β-oxidation genes PPARα and CPT1a were decreased. These data suggest that DUSP12 deficiency contributes to HFD-induced hepatic steatosis.

ASK1 is a MAPK kinase kinase that was identified as an activator of the MKK4/7–JNK and MKK3/6–p38 pathways, resulting in apoptosis.[33,34] Recently, a large number of studies have indicated a critically

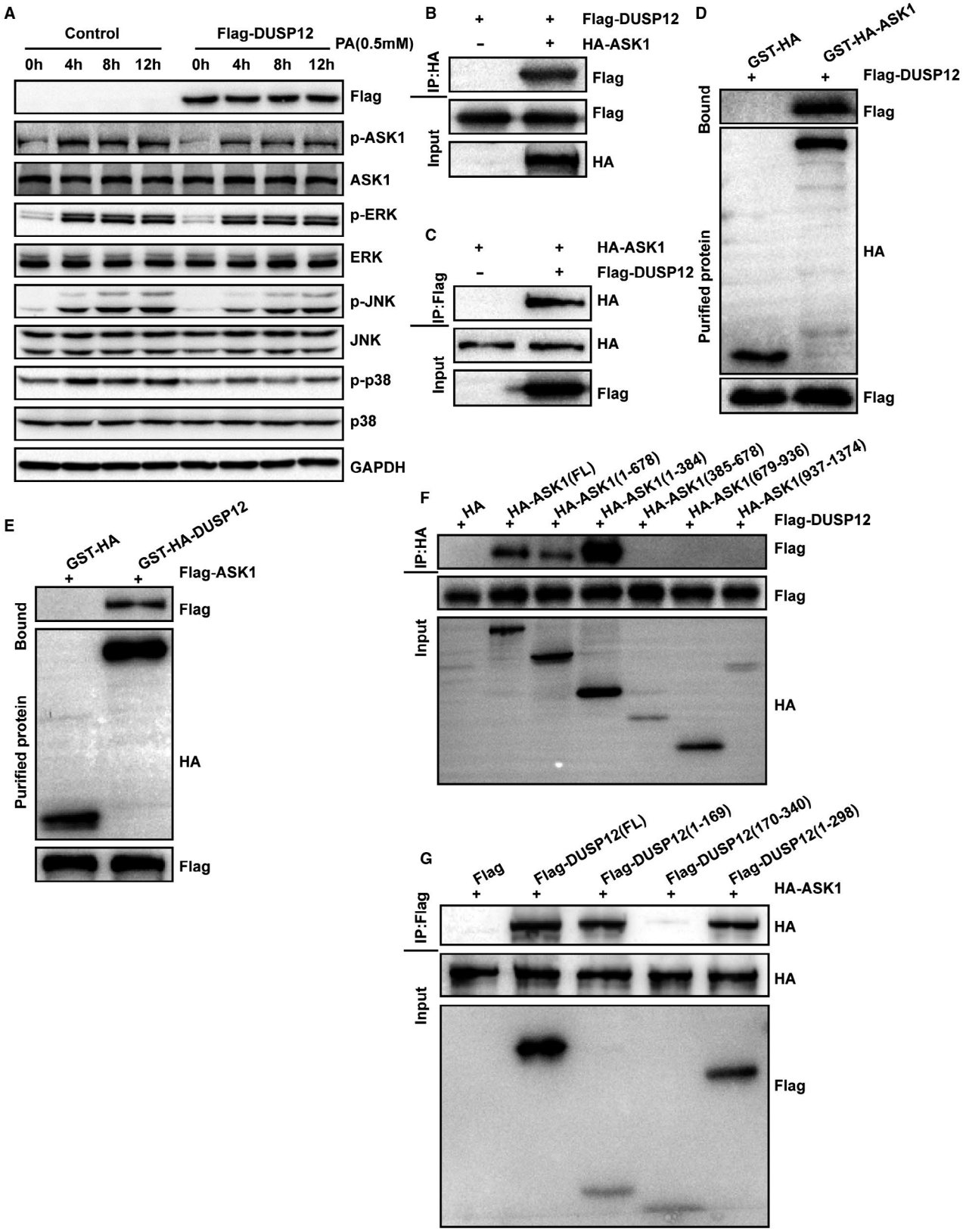
A
Control
Flag-DUSP12
PA(0.5mM)
0h 4h 8h 12h 0h 4h 8h 12h
Flag
p-ASK1
ASK1
p-ERK
ERK
p-JNK
JNK
p-p38
p38
GAPDH
B
+ + Flag-DUSP12
- + HA-ASK1
IP:HA
Flag
Flag
Input
HA
C
+ + HA-ASK1
- + Flag-DUSP12
IP:Flag
HA
HA
Input
Flag
D
GST-HA
GST-HA-ASK1
+ + Flag-DUSP12
Bound
Flag
Purified protein
HA
Flag
E
GST-HA
GST-HA-DUSP12
+ + Flag-ASK1
Bound
Flag
Purified protein
HA
Flag
F
+ HA
+ HA-ASK1(FL)
+ HA-ASK1(1-678)
+ HA-ASK1(1-384)
+ HA-ASK1(385-678)
+ HA-ASK1(679-936)
+ HA-ASK1(937-1374)
+ Flag-DUSP12
IP:HA
Flag
Flag
Input
HA
G
Flag
Flag-DUSP12(FL)
Flag-DUSP12(1-169)
Flag-DUSP12(170-340)
Flag-DUSP12(1-298)
+ + + + + HA-ASK1
IP:Flag
HA
HA
Input
Flag

FIG. 7. DUSP12 directly binds to ASK1 and inhibits its phosphorylation. (A) Activation of the ASK1 signaling pathway was measured in L02 cells transfected with Flag-DUSP12 at different times with 0.5 mM PA (n = 3 independent experiments). (B,C) 293T cells were transiently transfected with Flag-DUSP12 and HA-ASK1, and western blotting was used to detect the interaction between DUSP12 and ASK1. (D,E) GST precipitation assays showing direct DUSP12–ASK1 binding. Purified GST was used as a control. (F,G) The binding domains of DUSP12 and ASK1 were explored using full-length and truncated DUSP12 and ASK1 expression constructs and co-IP assays followed by western blotting. Abbreviations: ERK, extracellular signal-regulated kinase; FL, full-length; GAPDH, glyceraldehyde 3-phosphate dehydrogenase.

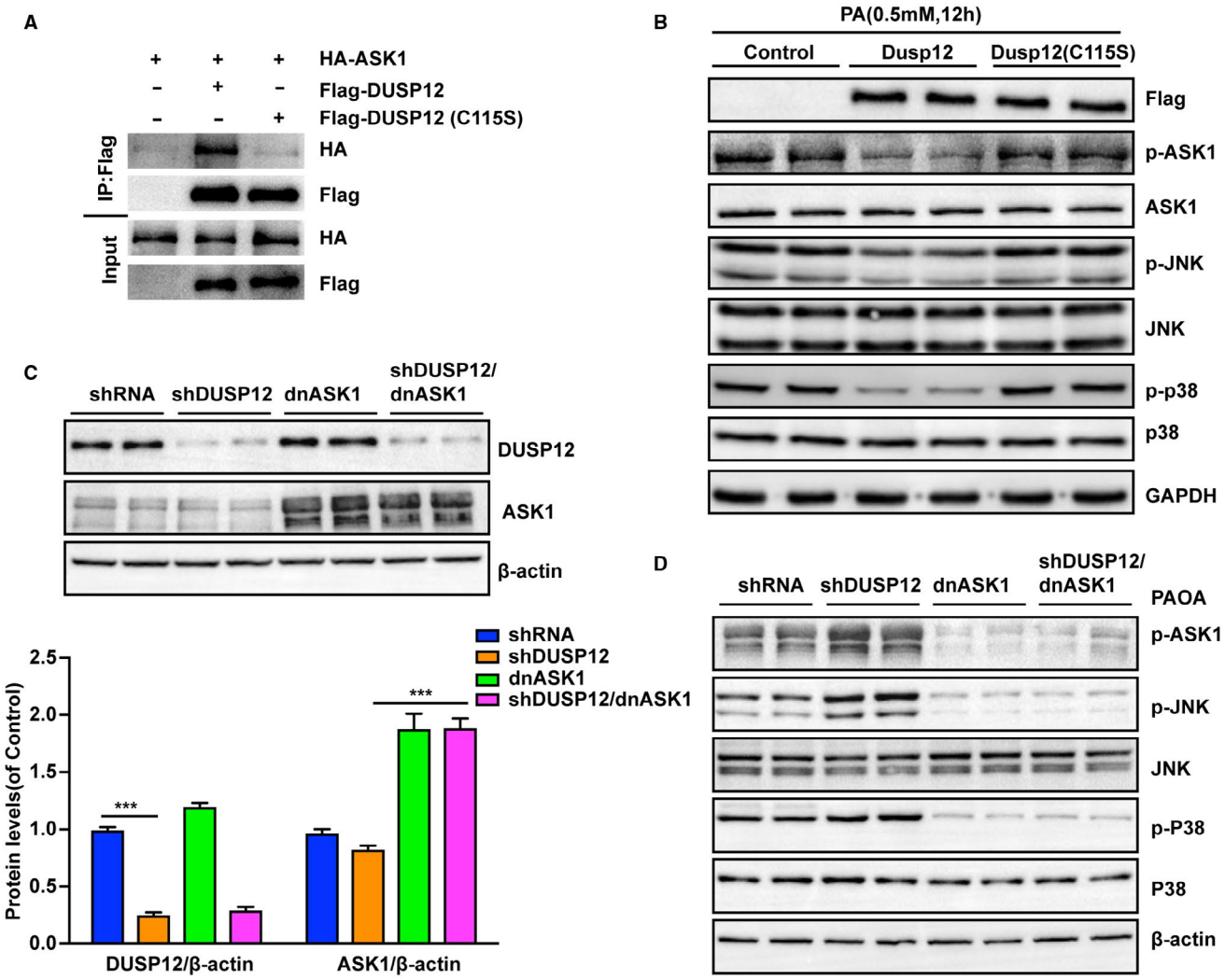

FIG. 8. ASK1 contributes to DUSP12-regulated lipogenesis and inflammation. (A) The interaction of DUSP12(WT), DUSP12 (C115S), and ASK1 in 293T cells. Cell lysates were precleaned and then subjected to IP with anti-Flag. The bound DUSP12 was determined by western blotting using anti-Flag antibodies. (B) Protein levels of phosphorylated and total ASK1, JNK and P38 were tested by western blotting in L02 cells that were transfected with DUSP12 and DUSP12 (C115S). (C) Protein levels of ASK1 and DUSP12 in L02 cells infected with different lentiviruses. (D) MAPK signaling activation was measured from the total and phosphorylated JNK and P38 levels in L02 cells in specific groups. Protein expression was normalized to that of β-actin. (E,F) Representative oil red O staining (E) and relative intracellular triglyceride levels (F) of L02 cells infected with the indicated lentivirus followed by PA/OA stimulation (n = 10). (G,H) mRNA levels of lipogenesis-related genes (G) and proinflammatory genes (H) in the indicated groups. mRNA expression of target genes was normalized to that of β-actin. All data represent the mean ± SEM. $^{*}P < 0.05$, $^{**}P < 0.01$, $^{***}P < 0.001$. Abbreviations: dn, dominant negative; GAPDH, glyceraldehyde 3-phosphate dehydrogenase; sh, short hairpin; TG, triglyceride.

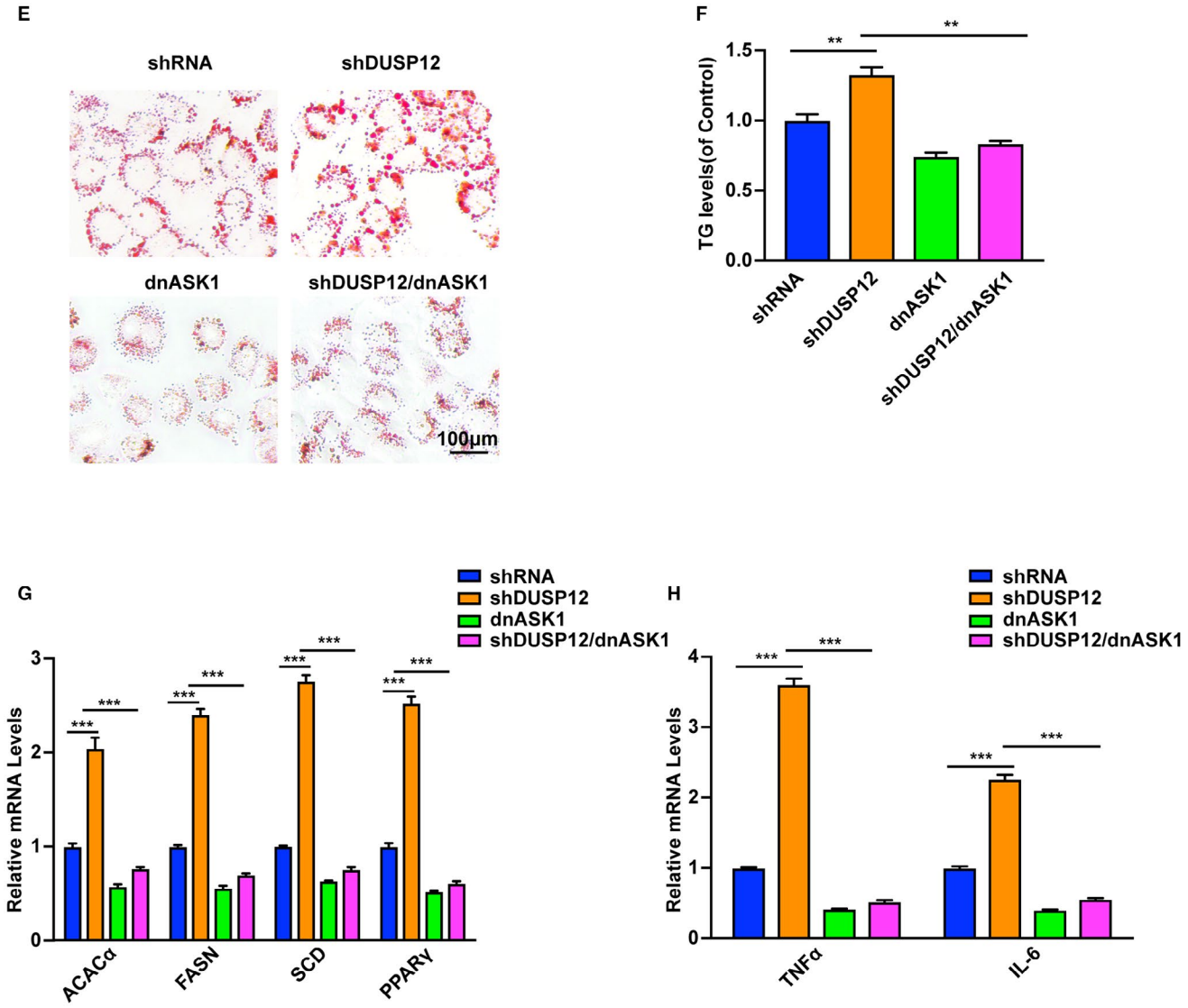

FIG. 8. *Continued.*

exacerbated role of ASK1 activation in the progression of NAFLD and NASH.[35-37] Importantly, hyperactivated ASK1 was detected in human subjects with NASH, which further supports the potential clinical use of ASK1 as a therapeutic target for NASH. In our study, we found that ASK1 activity was increased in the livers of DUSP12-CKO mice, whereas it was decreased in the livers of DUSP12-TG mice. More importantly, DUSP12 can directly interact with ASK1 and inhibit its activation, and blocking ASK1 activity abolished the effect of DUSP12 on hepatic steatosis, IR, and inflammation. Taken together, our results demonstrate that DUSP12 is a potential target for the treatment of NASH for its direct regulation of ASK1 activity.

ASK1 aggravates NASH progression primarily through its downstream targeting of JNK1. Studies have shown that JNK1 exacerbates NASH progression by reducing insulin sensitivity, impairing lipid homeostasis, and inducing inflammation simultaneously through its downstream factors.[38] JNK1 is markedly involved in lipid metabolism by regulating PPARα target genes[39,40] and promotes IR and glucose increase by accelerating insulin receptor substrate 1 serine phosphorylation.[41,42] Furthermore, a hyperactivated inflammatory answer can be triggered

by JNK through its downstream factors c-Jun and c-Fos, both of which bind to promoters of proinflammatory chemokines and cytokines.[43,44] Functionally, DUSP12 exerts its function in NAFLD/NASH by inhibiting lipid metabolic dysfunction while decreasing inflammation and improving IR by blocking the activation of ASK1 and the subsequent JNK1 pathway.

In summary, the present study establishes the molecular crosstalk between DUSP12 and ASK1 in the regulation of lipid metabolism and the progression of NAFLD. Approaches that improve lipid metabolism by manipulating a more distal molecule, such as increasing DUSP12 expression and activity, might rebalance lipid uptake and improve insulin sensitivity, thus making DUSP12 an attractive drug target for metabolic disorders such as liver steatosis, T2DM, myocardiopathy, and lipogenesis-related diseases.

REFERENCES

1) Kosmalski M, Mokros L, Kuna P, Witusik A, Pietras T. Changes in the immune system—the key to diagnostics and therapy of patients with non-alcoholic fatty liver disease. Cent Eur J Immunol 2018;43:231-239.
2) Ozturk A, Grajo JR, Gee MS, Benjamin A, Zubajlo RE, Thomenius KE, et al. Quantitative hepatic fat quantification in non-alcoholic fatty liver disease using ultrasound-based techniques: a review of literature and their diagnostic performance. Ultrasound Med Biol 2018;44:2461-2475.
3) Qin S, Wang S, Wang X, Wang J. Non-alcoholic fatty liver disease and the risk of urolithiasis: a systematic review and meta-analysis. Medicine (Baltimore) 2018;97:e12092.
4) **Wang JZ**, **Cao HX**, Chen JN, Pan Q. PNPLA3 rs738409 underlies treatment response in nonalcoholic fatty liver disease. World J Clin Cases 2018;6:167-175.
5) Tomic D, Kemp WW, Roberts SK. Nonalcoholic fatty liver disease: current concepts, epidemiology and management strategies. Eur J Gastroenterol Hepatol 2018;30:1103-1115.
6) Yao H, Qiao YJ, Zhao YL, Tao XF, Xu LN, Yin LH, et al. Herbal medicines and nonalcoholic fatty liver disease. World J Gastroenterol 2016;22:6890-6905.
7) Golabi P, Bush H, Stepanova M, Locklear CT, Jacobson IM, Mishra A, et al. Liver transplantation (LT) for cryptogenic cirrhosis (CC) and nonalcoholic steatohepatitis (NASH) cirrhosis: data from the Scientific Registry of Transplant Recipients (SRTR): 1994 to 2016. Medicine (Baltimore) 2018;97:e11518.
8) **Li Q**, **Dhyani M**, Grajo JR, Sirlin C, Samir AE. Current status of imaging in nonalcoholic fatty liver disease. World J Hepatol 2018;10:530-542.
9) Schwenger KJP, Bolzon CM, Li C, Allard JP. Non-alcoholic fatty liver disease and obesity: the role of the gut bacteria. Eur J Nutr 2018; https://doi.org/10.1007/s00394-018-1844-5. [Epub ahead of print]
10) Knebel B, Lehr S, Hartwig S, Haas J, Kaber G, Dicken HD, et al. Phosphorylation of sterol regulatory element-binding protein (SREBP)-1c by p38 kinases, ERK and JNK influences lipid metabolism and the secretome of human liver cell line HepG2. Arch Physiol Biochem 2014;120:216-227.
11) Zhang F, Zhang Z, Kong D, Zhang X, Chen L, Zhu X, et al. Tetramethylpyrazine reduces glucose and insulin-induced activation of hepatic stellate cells by inhibiting insulin receptor–mediated PI3K/AKT and ERK pathways. Mol Cell Endocrinol 2014;382:197-204.
12) Yang SQ, Lin HZ, Mandal AK, Huang J, Diehl AM. Disrupted signaling and inhibited regeneration in obese mice with fatty livers: implications for nonalcoholic fatty liver disease pathophysiology. Hepatology 2001;34:694-706.
13) Kozarova A, Hudson JW, Vacratsis PO. The dual-specificity phosphatase hYVH1 (DUSP12) is a novel modulator of cellular DNA content. Cell Cycle 2011;10:1669-1678.
14) Tilley DG, Sabri A. DUSPs as critical regulators of cardiac hypertrophy. Clin Sci (Lond) 2017;131:155-158.
15) **MacKeigan JP**, **Murphy LO**, Blenis J. Sensitized RNAi screen of human kinases and phosphatases identifies new regulators of apoptosis and chemoresistance. Nat Cell Biol 2005;7:591-600.
16) **Bonham CA**, **Steevensz AJ**, Geng Q, Vacratsis PO. Investigating redox regulation of protein tyrosine phosphatases using low pH thiol labeling and enrichment strategies coupled to MALDI-TOF mass spectrometry. Methods 2014;65:190-200.
17) Hu C, Zhang R, Wang C, Ma X, Wang J, Bao Y, et al. Lack of association between genetic polymorphisms within DUSP12-ATF6 locus and glucose metabolism related traits in a Chinese population. BMC Med Genet 2011;12:3.
18) **Cho SSL**, **Han J**, James SJ, Png CW, Weerasooriya M, Alonso S, et al. Dual-specificity phosphatase 12 targets p38 MAP kinase to regulate macrophage response to intracellular bacterial infection. Front Immunol 2017;8:1259.
19) **Li WM**, **Zhao YF**, Zhu GF, Peng WH, Zhu MY, Yu XJ, et al. Dual specific phosphatase 12 ameliorates cardiac hypertrophy in response to pressure overload. Clin Sci (Lond) 2017;131:141-154.
20) Wang XS, Diener K, Jannuzzi D, Trollinger D, Tan TH, Lichenstein H, et al. Molecular cloning and characterization of a novel protein kinase with a catalytic domain homologous to mitogen-activated protein kinase kinase kinase. J Biol Chem 1996;271:31607-31611.
21) Choi RY, Ham JR, Lee MK. Esculetin prevents non-alcoholic fatty liver in diabetic mice fed high-fat diet. Chem Biol Interact 2016;260:13-21.
22) Marin V, Rosso N, Dal Ben M, Raseni A, Boschelle M, Degrassi C, et al. An animal model for the juvenile non-alcoholic fatty liver disease and non-alcoholic steatohepatitis. PLoS One 2016;11:e0158817.
23) Yan H, Gao YQ, Zhang Y, Wang H, Liu GS, Lei JY. Chlorogenic acid alleviates autophagy and insulin resistance by suppressing JNK pathway in a rat model of nonalcoholic fatty liver disease. J Biosci 2018;43:287-294.
24) Ward M, Nguyen P, Akintorin S, Arcia R, Soyemi K. Interventions to improve liver enzyme screening testing in obese patients aged <18 years in a public hospital, Chicago, IL, 2017-2018. Pediatric Health Med Ther 2019;10:1-4.
25) Ogawa Y, Imajo K, Honda Y, Kessoku T, Tomeno W, Kato S, et al. Palmitate-induced lipotoxicity is crucial for the pathogenesis of nonalcoholic fatty liver disease in cooperation with gut-derived endotoxin. Sci Rep 2018;8:11365.
26) Weinstein AA, de Avila L, Paik J, Golabi P, Escheik C, Gerber L, et al. Cognitive performance in individuals with nonalcoholic fatty liver disease and/or type 2 diabetes mellitus. Psychosomatics 2018;59:567-574.
27) Gao Y, Wang YC, Lu CQ, Zeng C, Chang D, Ju S. Correlations between the abdominal fat–related parameters and severity of coronary artery disease assessed by computed tomography. Quant Imaging Med Surg 2018;8:579-587.

28) Mohlenberg M, Terczynska-Dyla E, Thomsen KL, George J, Eslam M, Gronbaek H, et al. The role of IFN in the development of NAFLD and NASH. Cytokine 2018; https://doi.org/10.1016/j.cyto.2018.08.013. [Epub ahead of print]
29) Cain EL, Braun SE, Beeser A. Characterization of a human cell line stably over-expressing the candidate oncogene, dual specificity phosphatase 12. PLoS One 2011;6:e18677.
30) le Nguyen B, Diskin SJ, Capasso M, Wang K, Diamond MA, Glessner J, et al. Phenotype restricted genome-wide association study using a gene-centric approach identifies three low-risk neuroblastoma susceptibility loci. PLoS Genet 2011;7:e1002026.
31) Mendez-Sanchez N, Cruz-Ramon VC, Ramirez-Perez OL, Hwang JP, Barranco-Fragoso B, Cordova-Gallardo J. New aspects of lipotoxicity in nonalcoholic steatohepatitis. Int J Mol Sci 2018;19:E2034.
32) Pierantonelli I, Svegliati-Baroni G. Nonalcoholic fatty liver disease: basic pathogenetic mechanisms in the progression from NAFLD to NASH. Transplantation 2018;103:e1-e13.
33) **Amos LA**, **Ma FY**, Tesch GH, Liles JT, Breckenridge DG, Nikolic-Paterson DJ, et al. ASK1 inhibitor treatment suppresses p38/JNK signalling with reduced kidney inflammation and fibrosis in rat crescentic glomerulonephritis. J Cell Mol Med 2018;22:4522-4533.
34) Zhu L, Yi X, Zhao J, Yuan Z, Wen L, Pozniak B, et al. Betulinic acid attenuates dexamethasone-induced oxidative damage through the JNK-P38 MAPK signaling pathway in mice. Biomed Pharmacother 2018;103:499-508.
35) **Sun P**, **Zeng Q**, **Cheng D**, Zhang K, Zheng J, Liu Y, et al. Caspase recruitment domain protein 6 protects against hepatic steatosis and insulin resistance by suppressing apoptosis signal-regulating kinase 1. Hepatology 2018;68:2212-2229.
36) **Xiang M**, **Wang PX**, **Wang AB**, Zhang XJ, Zhang Y, Zhang P, et al. Targeting hepatic TRAF1-ASK1 signaling to improve inflammation, insulin resistance, and hepatic steatosis. J Hepatol 2016;64:1365-1377.
37) Qu Y, Liu Y, Chen L, Zhu Y, Xiao X, Wang D, et al. Nobiletin prevents cadmium-induced neuronal apoptosis by inhibiting reactive oxygen species and modulating JNK/ERK1/2 and Akt/mTOR networks in rats. Neurol Res 2018;40:211-220.
38) Gan LT, Van Rooyen DM, Koina ME, McCuskey RS, Teoh NC, Farrell GC. Hepatocyte free cholesterol lipotoxicity results from JNK1-mediated mitochondrial injury and is HMGB1 and TLR4-dependent. J Hepatol 2014;61:1376-1384.
39) Vernia S, Cavanagh-Kyros J, Garcia-Haro L, Sabio G, Barrett T, Jung DY, et al. The PPARalpha-FGF21 hormone axis contributes to metabolic regulation by the hepatic JNK signaling pathway. Cell Metab 2014;20:512-525.
40) **Lu Y**, **Liu X**, **Jiao Y**, Xiong X, Wang E, Wang X, et al. Periostin promotes liver steatosis and hypertriglyceridemia through downregulation of PPARalpha. J Clin Invest 2014;124:3501-3513.
41) Schultze SM, Hemmings BA, Niessen M, Tschopp O. PI3K/AKT, MAPK and AMPK signalling: protein kinases in glucose homeostasis. Expert Rev Mol Med 2012;14:e1.
42) Aguirre V, Werner ED, Giraud J, Lee YH, Shoelson SE, White MF. Phosphorylation of Ser307 in insulin receptor substrate-1 blocks interactions with the insulin receptor and inhibits insulin action. J Biol Chem 2002;277:1531-1537.
43) Kodama Y, Brenner DA. c-Jun N-terminal kinase signaling in the pathogenesis of nonalcoholic fatty liver disease: multiple roles in multiple steps. Hepatology 2009;49:6-8.
44) Cazanave SC, Mott JL, Elmi NA, Bronk SF, Werneburg NW, Akazawa Y, et al. JNK1-dependent PUMA expression contributes to hepatocyte lipoapoptosis. J Biol Chem 2009;284:26591-26602.

Author names in bold designate shared co-first authorship.

Supporting Information

Additional Supporting Information may be found at onlinelibrary.wiley.com/doi/10.1002/hep.30597/suppinfo.